frontiers | Frontiers in Mechanical Engineering

ORIGINAL RESEARCH
published: 16 June 2022
doi: 10.3389/fmech.2022.921826

Surface Mo or Ni-Enrichment Applied to Granulated Self-Lubricating Composites: Microstructural and Tribological Evaluation

Keli Vanessa Salvador Damin[1,2], *Gabriel da Rosa Tasior*[1], *Gisele Hammes*[1], *Aloisio Nelmo Klein*[1], *José Daniel Biasoli de Mello*[1,3]*, *Tatiana Bendo*[1] and *Cristiano Binder*[1]

[1]Mechanical Engineering Department, Federal University of Santa Catarina, Florianópolis, Brazil, [2]Mechanical Department, Federal Institute of Santa Catarina, Chapecó, Brazil, [3]College of Mechanical Engineering, Federal University of Uberlândia, Uberlândia, Brazil

Sintered self-lubricating components may present inappropriate mechanical properties despite their excellent tribological properties. In general, alloying elements are used to improve these properties, but with a cost increase. As an alternative, surface enrichment (or surface alloying) with alloying elements may be applied. This study developed and characterized sintered composite materials surface-enriched with nickel or molybdenum. The results showed that the surface enrichment process is useful for increasing the tribomechanical properties. The Mo-enriched samples presented superior tribological results. Compared with the reference samples (not enriched), the Mo-enriched specimens showed an increase of 4,954% in scuffing resistance, lower friction coefficient (0.09), and reduced wear rate (68% and 96% lower for the specimen and the counter body). These results were mainly attributed to microstructural modification.

Keywords: powder metallurgy, surface alloying, tribology, microstructure. wear rate, scuffing resistance

OPEN ACCESS

Edited by:
Valentin L. Popov,
Technical University of Berlin, Germany

Reviewed by:
Prasanta Sahoo,
Jadavpur University, India
Jeng Haur Horng,
National Formosa University, Taiwan

***Correspondence:**
José Daniel Biasoli de Mello
d.mello@labmat.ufsc.br
ltm-demello@ufu.br

Specialty section:
This article was submitted to Tribology, a section of the journal Frontiers in Mechanical Engineering

Received: *16 April 2022*
Accepted: *05 May 2022*
Published: *16 June 2022*

Citation:
Damin KVS, Tasior GdR, Hammes G, Klein AN, de Mello JDB, Bendo T and Binder C (2022) Surface Mo or Ni-Enrichment Applied to Granulated Self-Lubricating Composites: Microstructural and Tribological Evaluation. Front. Mech. Eng 8:921826. doi: 10.3389/fmech.2022.921826

INTRODUCTION

With the current importance of economic and environmental aspects for maintaining a more sustainable society, issues related to friction and wear have been gaining increasing attention (Holmberg et al., 2014; Holmberg, Erdemir, 2017).

When service conditions become unfavorable or very severe, for instance, in cases of high-vacuum conditions, extreme temperatures and high speed and/or intense load, or in medical, pharmaceutical, or food processing equipment, liquid lubrication cannot be applied and solid lubrication is an alternative option (Stachowiak and Batchelor, 2001; Miyoshi, 2001; Miyoshi, 2007; Erdemir, 2015; Zhu et al., 2020).

Solid lubricants can be roughly defined as materials providing a dry friction coefficient below 0.2 and a wear rate of the order of $l0^{-6}$ mm^3/N.m (Miyoshi, 2001). There are two ways to incorporate a solid lubricant into a component: in the form of films (or coatings) (Erdemir, 2001; Donnet and Erdemir, 2008; Velkavrh et al., 2008; Donnet and Erdemir, 2008; Erdemir, 2015; Argibay et al., 2018 or as particles dispersed in the entire volume of the component (De Mello et al., 2010; Tang et al., 2011; Mahathanabodee et al., 2014; De Mello et al., 2017).

Self-lubricating composites are produced by powder metallurgy methods, mainly using uniaxial die pressing, the most economical and commonly used processing route (Thummler, Oberacker, 1993; De Mello et al., 2010; Mahathanabodee et al., 2014), and have been commercially consolidated

for many decades. Metals, ceramics, and polymers are all used as matrix materials, and graphite, fluorides, nitrides, sulfides, or polytetrafluoroethylene (PTFE) are the most common solid lubricants.

Given the higher strength, low cost, and wide availability (Teisanu and Gheorghe, 2011) of iron powders and iron-based sintered tribomaterials as a whole, the use of high-performance iron-based self-lubricating composites, in particular, has grown substantially, even superseding the use of copper-based tribomaterials (Dhanasekaran and Gnanamoorthy, 2007; Yilmaz et al., 2010; Merie et al., 2011; Ünlü, 2011; De Mello et al., 2013; Scharf, Prasad, 2013; Campos et al., 2015; Schroeder et al., 2015; Sharma, Anand, 2016). Structural parameters, in particular the degree of continuity of the metallic matrix associated with the content, size, and size distribution of the solid lubricant (Huang et al., 2009; Zhu et al., 2011; Reeves et al., 2015) and the mean free path between the solid lubricant particles combined with mechanical matrix properties, are at the origin of the high mechanical and tribological performance.

One of the most common solid lubricants used in producing iron-based self-lubricating composites in this manufacturing method is graphite, which presents a low coefficient of friction (COF) and very high thermal stability (Erdemir, 2001; Miyoshi, 2001; Stachowiak and Batchelor, 2001; Miyoshi, 2007; Erdemir, 2015; Su et al., 2017). However, traditional iron-based matrix self-lubricating composites usually need a large amount of graphite (>20%), and this represents a problem in conventional powder metallurgy techniques.

A parameter that requires special attention is the dispersion of the particles in the composite volume. In the classical method, for example, mixing of the solid lubricant particles with matrix powders, the solid lubricant spreads between the powder particles of the metal matrix, leading to unsatisfactory packing (Binder et al., 2008). Consequently, a discontinuous metallic matrix and, ultimately, low mechanical strength are observed due to the layers of the insoluble solid lubricant, which hampers the contact between the particles during sintering (Wu et al., 1997; Yas' et al., 1976; Teisanu and Gheorghe, 2011; Binder et al., 2016; Omrani et al., 2017; Furlan et al., 2018; Hammes et al., 2017).

To prepare self-lubricating components with a controlled microstructure, three main approaches can help overcome these difficulties. The first is based on the capillary action of a liquid phase. The liquid phase spreads and penetrates the interfaces by capillarity, thus carrying the solid lubricant particles and rearranging them in discrete agglomerates (De Mello et al., 2017). The second case, recently introduced by our group (De Mello et al., 2010; De Mello et al., 2013; Campos et al., 2015; De Mello et al., 2017), has proven to be remarkably efficient in obtaining high tribological (dry friction coefficient = 0.04; wear rate = $8.28.10^{-6}$ mm^3. $N^{-1}.m^{-1}$) and mechanical (ultimate tensile strength = 800 MPa; elongation 6.3%) performance. In this processing route, solid lubricant reservoirs are generated *in situ* during sintering by decomposing a precursor, giving rise to a more continuous matrix.

The granulation process (Ma et al., 2015; Demetrio et al., 2017; Mônego et al., 2018; Damin, 2019), which is the third approach, not only avoids the spread of the solid lubricant between the powder particles of the metal matrix but also creates a barrier between the graphite and ferrous matrix, thus effectively avoiding diffusion of carbon into the matrix (Mônego et al., 2018; Damin, 2019). The granulation process can be defined as the intentional agglomeration of fine particles (powders) by adding water or a binder solution to form agglomerates with controlled sizes called granules (Reed, 1998). This process makes it possible to use more than one powder and thus produce granules with specific properties (Bernardes, 2006).

One way to obtain sintered ferrous matrix composites with high mechanical strength is to use alloying elements (Thummler and Oberacker, 1993; Dhanasekaran and Gnanamoorthy, 2007). However, the use of these alloying elements will increase the processing complexity due to additional processes used to disperse them throughout the component volume, thus increasing the cost of the component. Therefore, it is necessary to promote the increase in wear resistance only on the component surface and thus avoid alloying elements in the entire volume. One way of economically achieving the desired microstructural change is by applying surface modification techniques. One such approach is plasma surface enrichment (Bendo et al., 2016; Pavanati et al., 2007), in which alloying elements are added from a reusable cathode onto the surface of the sintered component. The aim is to modify the chemical composition and microstructure on the surface and volume immediately below it, producing materials that are more resistant in the surface region and have longer functional life (Pavanati et al., 2007; Klein et al., 2013; Bendo et al., 2011). Furthermore, in addition to being an environmentally friendly process, the plasma enrichment co-occurs in the sintering step, without incurring additional processing costs (Bendo et al., 2011; Klein et al., 2013). Also, the process does not require high-cost pre-alloyed powders, which strongly influence the compressibility, dimensional variation, and homogenization during processing and sintering (German, 1996).

This investigation aimed to produce sintered self-lubricating composites using granulated solid lubricants and evaluate the microstructural modifications and tribological performance obtained with the surface enrichment of these composites with molybdenum or nickel.

MATERIALS AND METHODS

The surfaces of the specimens of the granulated self-lubricating composites produced by powder metallurgy were enriched with nickel or molybdenum using plasma technology. Hexagonal boron nitride (hBN) and graphite powders were used to produce the granulated particles. **Table 1** shows the details of the powders. Polyvinyl alcohol (PVA), supplied by Sigma Aldrich, was used as a binder. **Figure 1** shows a schematic flowchart describing the steps of the sample preparation.

The granulation process consisted of homogenizing the lubricants (hBN and graphite) in a Y mixer for 30 min,

TABLE 1 | Specifications of the powders used.

	Powder	Commercial name	Manufacturer	Particle size (μm)
Granules	hBN	AC 6004	Momentive	12–13
	Graphite	Micrograf 99,545 HF	Nacional de Grafite	20–45 (d-50)
Matrix	Iron	AHC 100.29	Höganäs	100 (d50)
	Graphite	UF4	Höganäs	<6.10 (d50)

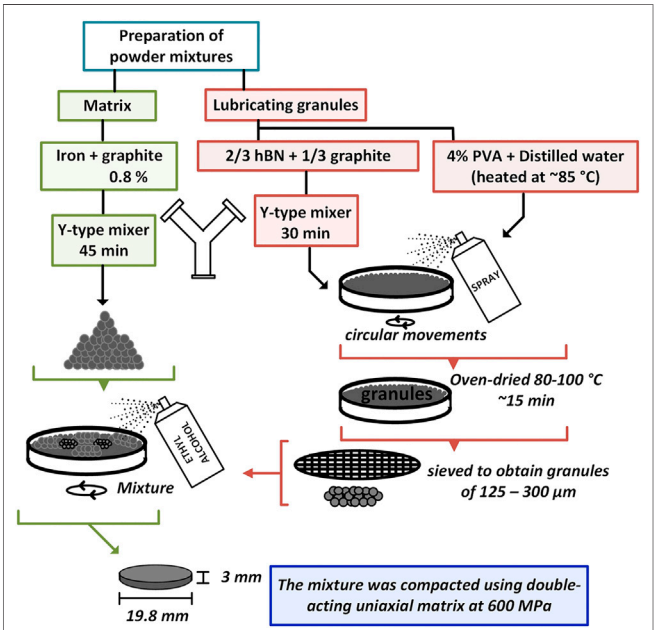

FIGURE 1 | Sample production schematic flow-process diagram.

without beads. A ratio of 1/3 of graphite to 2/3 of hBN was used. Concomitantly, an aqueous PVA solution (4 wt%, relative to the total mass of the lubricant) was prepared with distilled water (2.6X). The solution was heated (~85°C) in a magnetic stirrer (Nalgon–HOTLAB II) under stirring until complete dissolution of the polymer and then placed in a spray bottle.

The lubricant mixture was rotated on a bowl, while the aqueous PVA solution was sprayed onto the powders to form granules. This process was carried out until the powder mixture no longer absorbed the solution. The mixture was then oven-dried (De Leo–DL-SEDT) at 80–100°C for 10–15 min. After drying, the larger granules were separated and broken with a blade. These steps were repeated several times until the entire solution (PVA + water) was sprayed.

After drying, the granules were sieved (Bertel–VP-01) for 5 min, and the granular fraction (125–300 μm) was used to produce the self-lubricating sintered composite.

The metallic matrix was prepared using iron and carbon powders (details in **Table 1**), and the chemical composition of the specimens can be seen in **Table 2**.

Iron powder, graphite, and 0.8% amide were homogenized in a Y-type mixer (45 min, 35 rpm using ϕ= 3 mm and ZrO_2 balls). Due to its high degree of segregation in the mixing step, the granulated lubricant was added to the matrix powders immediately before compaction. The mixture was manually shaken after spraying with ethyl alcohol (p.a.) to facilitate agglutination of the granules with the powders of the matrix. The samples were compacted using a double-acting uniaxial matrix, applying a compacting pressure of 600 MPa. Cylindrical specimens (ϕ = 19.8 mm, h = 3 mm) were produced.

After compaction, the samples were sintered and simultaneously surface-enriched in a plasma reactor prepared in the laboratory (Hammes, 2006). The specimens were positioned on the anode and processed in a floating potential plasma in this process. Two groups of samples were enriched, one group with molybdenum and the other with nickel. For enrichment with Mo, the cathode used contained 99.4% Mo (TZM alloy). For enrichment with Ni, the cathode was produced with a Ni 200 alloy with 99.7% Ni. The samples subjected only to sintering were also prepared for comparison purposes. In this case, an AISI 1020 steel cathode was used. The parameters of the processing step and the sample designations are shown in **Table 3**.

The characterization of the samples included analysis of the surface and cross section by scanning electron microscopy (SEM) (TESCAN Vega 3), energy-dispersive X-ray spectroscopy (EDS) (Oxford x-act), and Vickers microhardness determination (Future-Tech FM-800) according to MPIF Standards 51 and 52 (Metal Powder Industry Federation, 2005; Metal Powder Industry Federation, 2010), with a load of 0.01 kg for 15 s. In addition, the surface was also analyzed by X-ray diffraction (XRD) (Philips X'Pert) using the Bragg–Brentano geometry and Cu–K_α radiation. Data from the JCPDS database were used to identify the phases from the positions of the

TABLE 2 | Chemical composition of samples.

Fe (matrix) (%w)	C (matrix) (%w)	C (granulate) (%v)	hBN (granulate) (%v)
Balance	0.6	2.5	5.0

TABLE 3 | Parameters of the sintering and surface enrichment processes.

Designation	Condition	Temperature (°C)	Time (min)	Pulse active time (μs)	Pressure (Pa)	Output voltage (v)	Gas composition (%)	Gas flow (cm^3/tin)
S.G	Sintered	1,150	60	20	133×10^2	400	$5H_2$/95Ar	4×10^{-6}
Mo.G	Sintered Mo enriched	1,150	60	150	2.66×10^2	500	$20H_2$/80Ar	4×10^{-6}
Ni.G	Sintered Ni enriched	1,150	60	150	333×10^2	600	$20H_2$/80Ar	4×10^{-6}

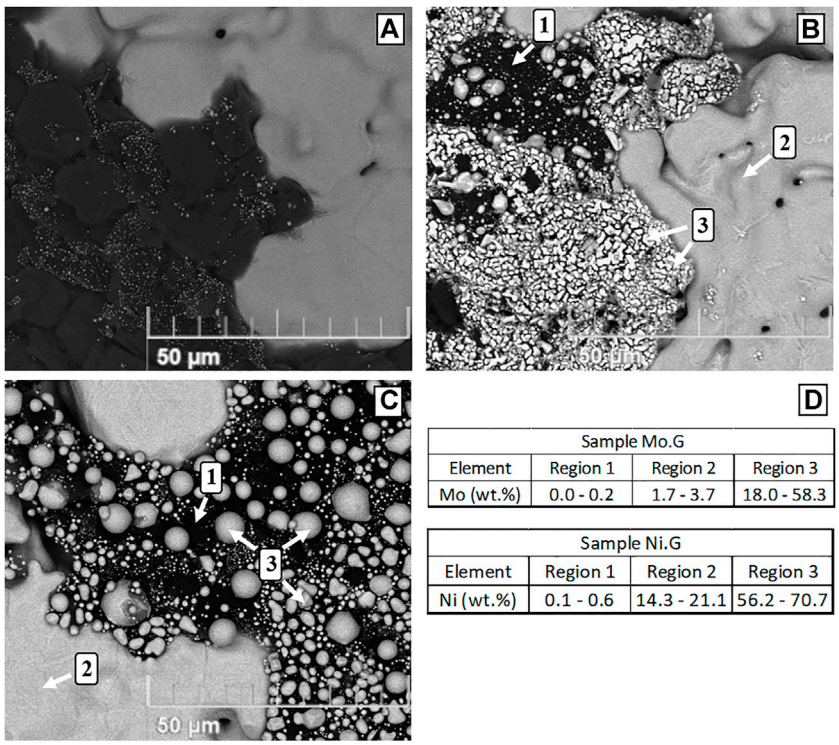

FIGURE 2 | SEM micrographs of typical surfaces **(A)** sample S.G–sintered only, **(B)** sample Mo.G–molybdenum-enriched, **(C)** sample Ni.G–nickel-enriched, and **(D)** EDS analysis results.

diffraction peaks (International Center for Diffraction Data, 2004).

The tribological properties were evaluated on a CETR UMT tribometer. In this analysis, two configurations were tested, both being sphere-on-plane under reciprocating sliding movement using a 5 mm diameter, with an AISI 52100 steel ball as the counter body, at a constant frequency (2 Hz) and stroke (10 mm). The first test configuration (incremental load tests) was performed as proposed by de Mello and Binder (De Mello and Binder, 2006) and had the objective of determining the scuffing resistance, defined as the work (N.m) carried out while the coefficient of friction (COF) remained below 0.2. At the same time, at least 190 s of permanence above this value was considered to establish this definition. The second test configuration (constant load tests) involved using a constant load of 7.0 N for 1 h and was used to evaluate the COF and wear rate of the specimen and counter body. At least four measurements were performed in all tribological tests for each condition. White light interferometry (Zygo NewView 7,300) was used to measure the sample wear volumes. Topographical data processing was carried out using MountainsMap Universal 7.1® software. For all the results obtained in this study, an evaluation to detect spurious values was performed using the Chauvenet criterion (Taylor, 1996).

RESULTS AND DISCUSSION

Figure 2 shows the typical surfaces of the specimens studied. The reference sample (sintered only, S.G) comprised granules of the

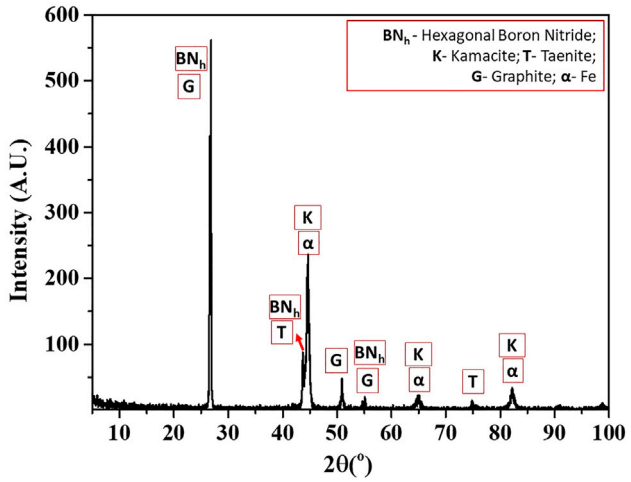

FIGURE 3 | X-ray diffraction pattern obtained from the surface of the Ni-G sample.

solid lubricants (dark phase) and the metallic matrix (light region), as seen in **Figure 2A** .

Regardless of the enrichment element (Mo or Ni), it can be observed that the enrichment occurred heterogeneously both in the matrix and solid lubricant reservoirs, generating the formation of three regions presenting different concentrations (**Figure 2B,C**). Region 1 within the lubricant reservoir corresponds to an area where the enrichment was minimal. In this region, for the Mo.G sample, the Mo concentration was 0.0–0.2 wt% Mo (**Figure 2D**) and for the Ni.G sample, the Ni concentration was 0.1–0.6 wt% (**Figure 2D**).

In region 3, the concentration ranges for the enrichment elements in the Mo.G and Ni.G samples were 18.0–58.3 wt% and 56.2–70.7 wt%, respectively. In the case of region 2, the Mo concentration in the Mo.G sample matrix was 1.7–3.7 wt%, increasing the hardenability (Teisanu and Gheorghe, 2011; Hammes al., 2017; Binder et al., 2016), while the concentration of Ni in the Ni.G sample was 14.3–21.1 wt%, which allowed the formation of kamacite and taenite phases, as observed in the X-ray diffraction patterns (**Figure 3**). The JCPDS cards used to identify the phases were as follows: 01-075-1,621 (graphite), 01-087-072 (α-Fe), 00,045 0895 (hBN), 00-037-0474 (kamacite), and 00-047-1,417 (taenite). Kamacite is a nickel-poor solid iron solution with a CCC structure and microhardness around 181 HV (Bralla, 1996; Al-Bassam, 1978). On the other hand, taenite is a nickel-deficient solid iron solution with a CFC structure and microhardness ranging from 350–500 HV, depending on the nickel content (Bralla, 1996; Al-Bassam, 1978; Bendo et al., 2014; Anthony et al., 2017).

Figure 4 shows microstructural aspects of the cross sections of the samples. The sintered sample S.G comprises perlite and ferrite (**Figure 4A**) as confirmed by the microhardness profile showing values between 150—250 HV (**Figure 5**).

The Mo-enriched layer (needle-like morphology between the arrows) of the Mo-enriched samples can be seen in **Figure 4B**. It has a thickness of 13.38 ± 2.67 μm and a molybdenum content between 2.4 and 0.9 wt% in the first 10 μm, as seen in the EDS results (**Figure 6**). Furthermore, according to **Figure 5**, the microhardness profile values were within the typical limits for bainite (~450–230 HV) (Clayton et al., 1987; Bhadeshia, 2001), thus corroborating the presence of this phase.

The microstructure of the Ni.G sample (**Figure 4C**) is complex, and two regions can be observed. It is assumed that the outermost region (I – thickness 4.88 ± 1.45 μm) is formed by taenite as it presents a high concentration of nickel (between 11.5–19.4 wt%) (**Figure 6**) and microhardness (340.8 ± 28.2 HV–**Figure 5**) according to the values reported for taenite (Al-Bassam, 1978; Xie, Chen, 2015; Anthony et al., 2017).

The inner region (II–thickness 7.29 ± 2.69 μm) has a low nickel concentration (0.3–9.3 wt%) (**Figure 6**) and microhardness (~250–200 HV–**Figure 5**), which is in agreement with the properties of kamacite (Al-Bassam, 1978; Xie, Chen, 2015).

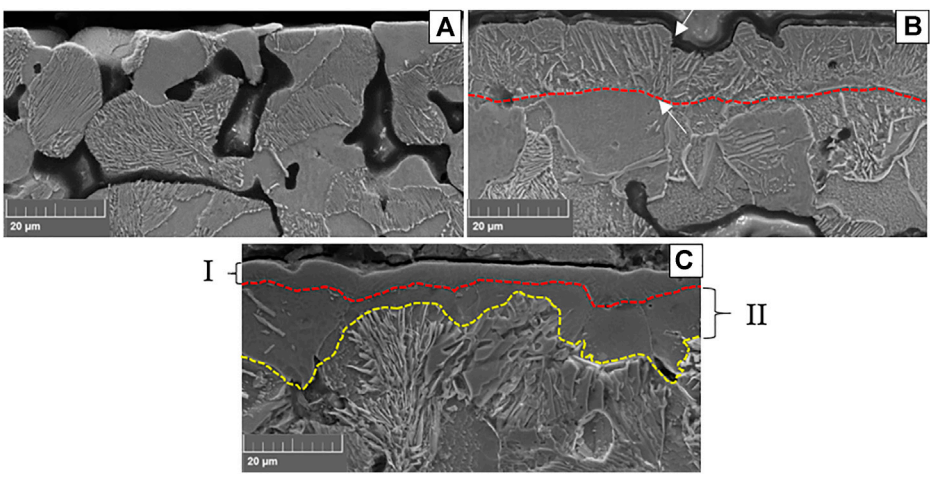

FIGURE 4 | SEM micrographs of cross sections of **(A)** the S.G sample, **(B)** Mo.G sample, and **(C)** Ni.G sample. Nital 2%.

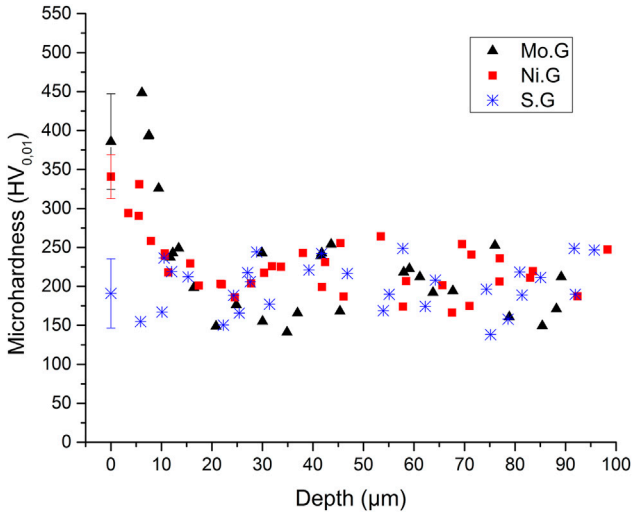

FIGURE 5 | Microhardness profiles (cross section) and the surface microhardness (0 μm) of the specimens.

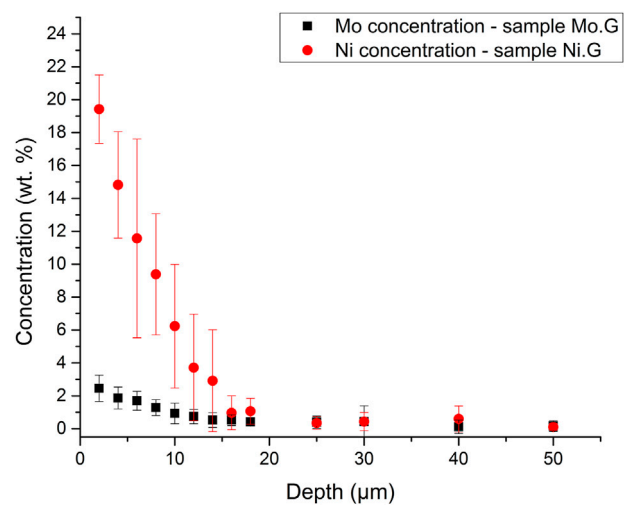

FIGURE 6 | Chemical composition profiles (EDS) of the cross section (error bars show standard deviation).

To evaluate how the enrichment process altered the tribological characteristics of the samples, the scuffing resistance, COF, and wear rate were determined. **Figure 7** shows the evolution of the COF during the incremental load tests. First, there is a transient region related to the beginning of contact between the counter body and specimen for all conditions. A high lubricity steady-state was then reached for the Mo.G sample. For the S.G and Ni.G specimens, after the transient region, the COF remains the same up to approximately 10 m. In the case of the S.G sample, it increases rapidly to values above the lubricity limit (0.2), while for the Ni.G sample, the COF remains between 0.15 and 0.2 up to a distance of 20 m. After this, the COF value increases rapidly.

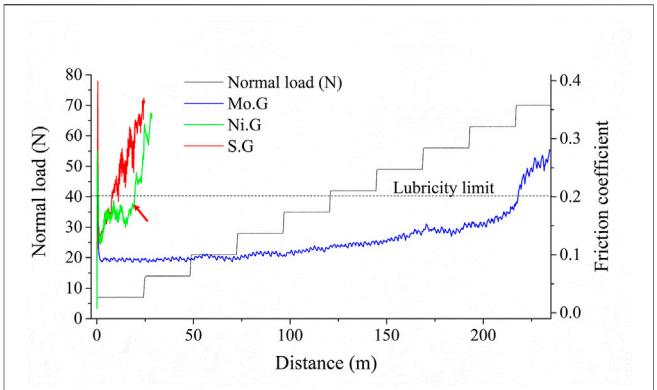

FIGURE 7 | Evolution of the COF and the normal load with the sliding distance.

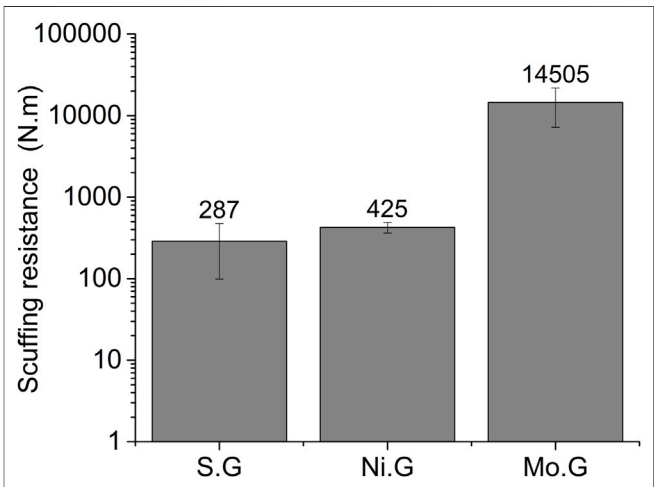

FIGURE 8 | Average scuffing resistance (error bars show standard deviation).

Figure 8 shows the average scuffing resistance. It can be observed that the sample enriched with molybdenum (Mo.G) showed a 4, 954% increase in scuffing resistance (14,505 N.m) compared to the non-enriched condition (287 N.m). The massive performance improvement may be associated with the presence of bainite, formed due to enrichment by molybdenum (**Figure 6**). Due to its greater hardness, bainite prevented premature plastic deformation of the matrix, even under high loads. This consequently hindered the sealing of solid lubricant reservoirs, promoting higher scuffing resistance, as previously reported (De Mello et al., 2013; Damin et al., 2019:; Damin et al., 2020).

The statistical analysis of the scuffing resistance of the Ni.G (425 N m ± 62 N m) and S.G (287 N m ± 188 N m) samples indicated that the two results are statistically identical, suggesting that nickel enrichment did not promote improvement in scuffing resistance. Furthermore, the same result was obtained by Damin (Damin et al., 2019) in the Ni-

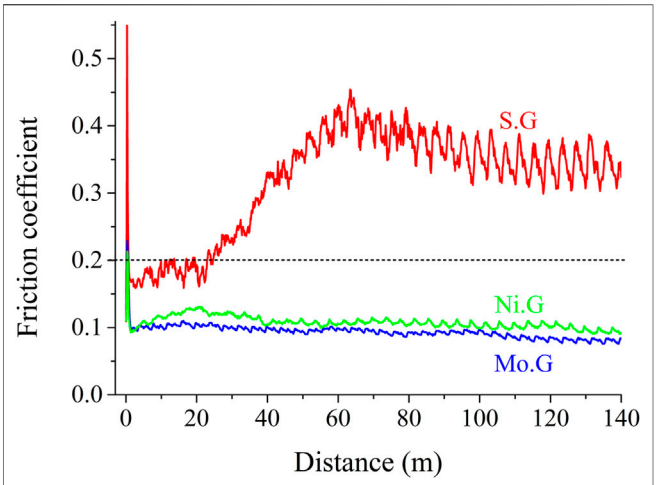

FIGURE 9 | Evolution of the COF in tests under constant normal load (7 N).

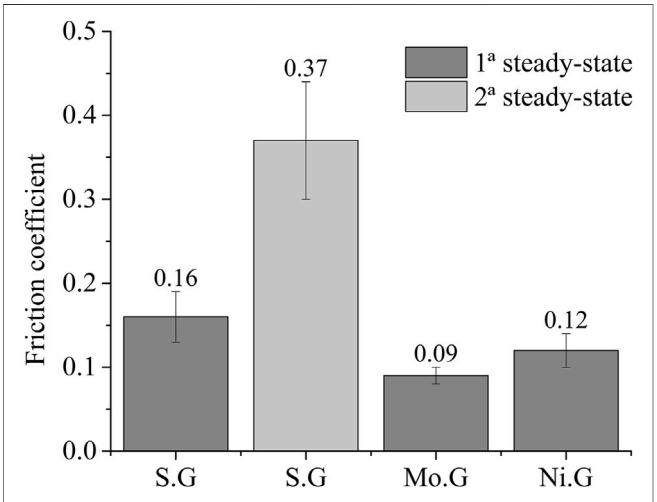

FIGURE 10 | Average steady-state COF (error bars show standard deviation).

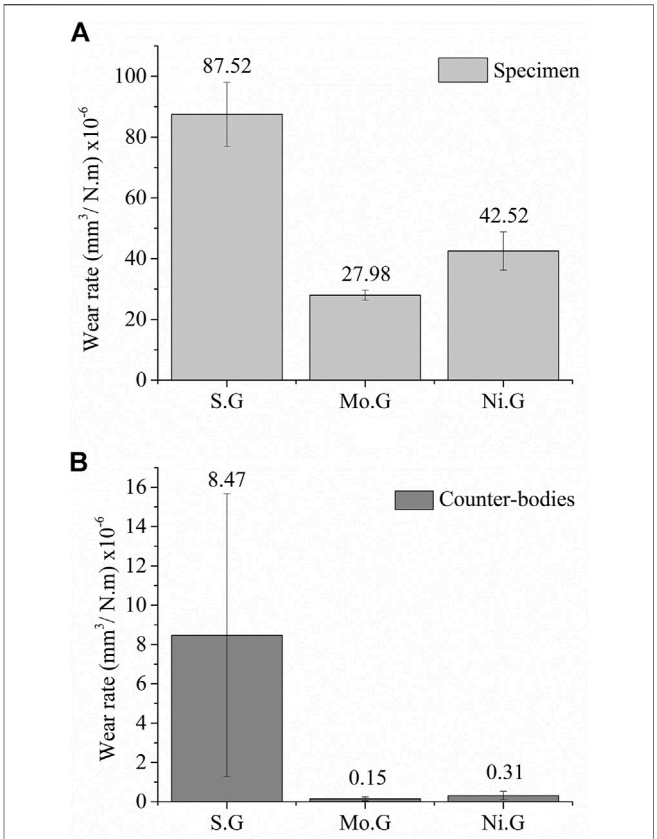

FIGURE 11 | Wear rates after reciprocating sliding tests: **(A)** specimens and **(B)** counter bodies.

enrichment of self-lubricating composites (Fe + 0.6C + 3SiC) produced by powder injection molding.

In addition, although enrichment promotes the formation of taenite (340.8 ± 28.2 HV), which is more resistant than kamacite (~250–200 HV–**Figure 5**), the taenite formed has less thickness (4.88 ± 1.45 μm). Thus, the action of the counter body quickly consumes it. Moreover, an increase in the COF can be observed in **Figure 7**, indicated by the red arrow, suggesting that the thin layer of taenite was consumed with consequent interaction with the less resistant kamacite.

The low scuffing resistance can, therefore, be explained by the hardness difference and the consequent ability to restrict the sealing of reservoirs (granules) of the solid lubricant of the active phase: ferrite and perlite for the S.G samples, bainite for the Mo.G samples, and taenite and kamacite for the Ni.G samples (**Figures 4**, **5**).

Figure 9 shows the evolution of the COF with the sliding distance during the constant load tests. The reference sample (S.G) showed two steady states. At the beginning of the test, the first state had a low value (0.16) retained until about 20 m of the sliding distance. After this point, the COF increased outside the lubricity region (0.37). This value remained until the end of the test, indicating a probable sealing of the granular lubricant due to the low mechanical resistance of the metal matrix to plastic deformation, as previously reported (Damin et al., 2020).

Surface enrichment affects lubricity. For Mo- and Ni-enriched specimens, the COF presented only one steady state, with average values of 0.09 and 0.12, respectively (**Figure 10**). The Mo-enriched samples showed reductions of 44% and 76% in the COF concerning the first and second steady state of the S.G samples, and these values were 25% and 67%, respectively, for the Ni-enriched samples.

Figure 11 shows how the surface enrichment reduced the wear rates of the samples and the respective counter bodies. The wear rate decreased from 87.52 ± 10.50 × 10–6 mm^3 N^{-1} m^{-1} for the S.G sample to 42.52 ± 6.29 × 10–6 mm^3 N^{-1} m^{-1} for the Ni. G sample and to 27.98 ± 1.69 × 10–6 mm^3 N^{-1} m^{-1} for the Mo.G sample (**Figure 11A**). This is equivalent to 51% and 68% reductions in the wear rate. There was also a reduction of >96% in the wear rate of the counter bodies of both enriched samples (**Figure 11B**). This figure also shows that the wear of the specimens controls the

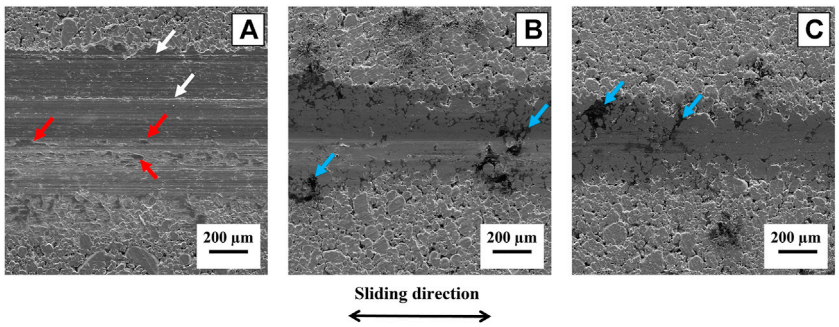

FIGURE 12 | SEM micrographs showing typical wear scars: **(A)** S.G, **(B)** Ni.G, and **(C)** Mo.G.

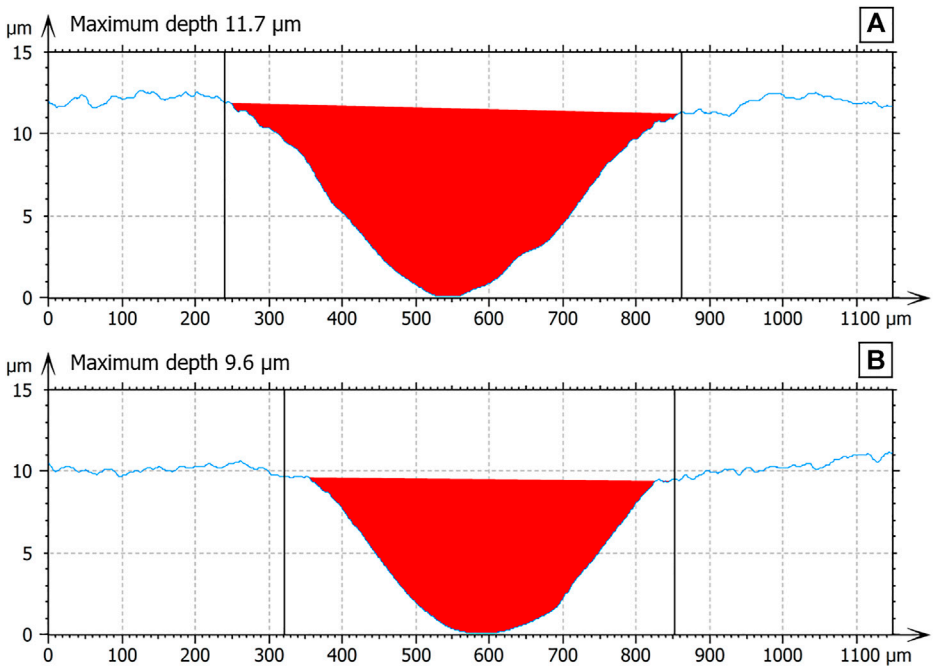

FIGURE 13 | Average cross-sectional profile of the wear track: **(A)** Ni.G and **(B)** Mo.G.

behavior of the system since the wear of the counter bodies is, as a rule, at least an order of magnitude lower. In addition, the wear rate of the nickel-enriched samples and respective counter bodies is around twice that of the samples enriched with molybdenum.

Figure 12 shows typical aspects of the wear marks after the constant load tests.

For the non-enriched composites (190.9 ± 44.4 HV–surface hardness), seen in **Figure 12A**, the wear mark is pronounced and uniformly wide. Also, there is total sealing of the solid lubricant reservoirs and evidence of abrasive wear (white arrows) and some small tribolayer islands randomly distributed (red arrows). The EDS results (not shown) revealed that these islands and the surrounding regions are oxygen-rich, which explains the greater wear and COF values. In contrast, the wear marks of the enriched samples (**Figures 4B,C**), in addition to not showing evidence of abrasive wear, present variable width (a possible consequence of the heterogeneity of enrichment shown in **Figure 2**). In addition, regardless of the enrichment material, the results show active reservoirs of solid lubricants (granules) inside the wear mark (blue arrows) and thin oxygen and solid lubricant–rich tribolayers (evidenced by EDX, also not shown), which could explain the lower wear and friction coefficient of the pair.

Concerning the enriched samples, it was observed that the Mo.G sample had a lower wear rate, which was attributed to the higher hardness (385.8 ± 61.4 HV–surface hardness) and thickness (13.38 ± 2.67) of the bainitic microstructure that developed in the Mo-enriched sample (Mo.G) when compared to the Ni-enriched sample (Ni.G), in which the taenite had higher hardness (340.8 ± 28.2 HV) but lower thickness (4.88 ± 1.45 µm).

Consequently, during the wear test of the Ni.G sample, the kamacite phase of less hardness showed a higher wear rate (Al-Bassam, 1978.; Damin et al., 2019; Damin et al., 2020). This result is confirmed by the cross section profile of the sample wear track after the reciprocating sliding for 1 h at 7 N (**Figure 13**).

For the Ni.G sample (**Figure 13A**), the maximum wear depth (11.7 μm) was greater than the depth of taenite (4.88 μm ± 1.45 μm) and reached the kamacite phase. On the other hand, for the Mo.G sample (**Figure 13B**), it was observed that the maximum wear depth (9.6 μm) remained within the bainitic region.

CONCLUSION

The influence of nickel or molybdenum-surface enrichment on the microstructural and tribological properties of self-lubricating composites (granulated graphite (2.5%v) and hBN (5.0%v) in a Fe + 0.6C metallic matrix) produced by powder metallurgy was investigated. The following conclusions can be drawn:

1) The surface enrichment was efficient for the metallic matrix and solid lubricant reservoirs.
2) The Ni.G sample had a COF of 0.12 and showed a reduction in the wear rate of the specimen (51%) and the counter body (96%) compared to the reference sample (S.G).
3) The Mo.G sample showed the best tribological properties with a COF of 0.09. In addition, the scuffing resistance increased by 4, 954%, and the wear rate reduced by 68 and 96% for the specimen and the counter body, respectively. This result is attributed to minor wear and plastic deformation of the matrix, which reduced the sealing of the lubricant reservoirs, with an increase in the microhardness of the matrix due to the formation of bainite.

Finally, this study showed the possibility of producing self-lubricating composites with improved properties without adding alloying elements and a consequent decrease in cost and potential processing issues such as the segregation of powders during mixing.

DATA AVAILABILITY STATEMENT

The raw data supporting the conclusion of this article will be made available by the authors, without undue reservation.

AUTHOR CONTRIBUTIONS

KD was the principal investigator, supervised the production of the samples, carried out the experiments, described and co-analyzed the results, and wrote the first draft of the manuscript. GT helped in carrying out the experiments. GH helped design and supervise the whole project and contributed to the analysis of the results. AK designed the entire project, supervised the research, analyzed the results, and funding acquisition. JdM helped design the whole project, analyze the results, and had a major role in writing the final version of the manuscript and tribological evaluation. TB helped supervise the whole project and contributed to the analysis of the results. CB helped supervise the research, funding acquisition, and contributed to the analysis of the results.

ACKNOWLEDGMENTS

The authors acknowledge the following Brazilian agencies for funding this research: CNPq, CAPES, BNDES, PRH-ANP, UNIEDU Postgraduate program, and FINEP and Nidec/Embraco and IFSC for technical support.

REFERENCES

Al-Bassam, K. S. (1978). The Mineralogy and Chemistry of the Alta'ameem Meteorite. *Meteoritics* 13, 257–265. doi:10.1111/j.1945-5100.1978.tb00815.x

Anthony, J. W., Bideaux, R. W., Bladh, K. W., and Nichols, M. C. (2017). *Handbook of Mineralogy*. Chantilly: Mineralogical Society of America.

Argibay, N., Babuska, T. F., Curry, J. F., Dugger, M. T., Lu, P., Adams, D. P., et al. (2018). *In Situ* tribochemical Formation of Self-Lubricating Diamond-like Carbon Films. *Carbon* 138, 61–68. doi:10.1016/j.carbon.2018.06.006

Bendo, T., Maliska, A. M., Acuña, J. J. S., Binder, C., Consoni, D. R., et al. (2016). The Effect of Mo on the Characteristics of a Plasma Nitrided Layer of Sintered Iron. *Appl. Surf. Sci.* 363, 29–36. doi:10.1016/j.apsusc.2015.11.200

Bendo, T., Pavanati, H. C., Klein, A. N., Martinelli, A. E., and Maliska, A. M. (2011). Plasma Nitriding of Surface Mo-Enriched Sintered Iron. *ISRN Mater. Sci.* 2011, 1–8. doi:10.5402/2011/121464

Bendo, T., Maliska, A. M., Acuña, J. J. S., Binder, C., Demetrio, K. B., and Klein, A. N. (2014). Nitriding of Surface Mo-Enriched Sintered Iron: Structure and Morphology of Compound Layer. *Surf. Coat. Technol.* 258, 368–373. doi:10.1016/j.surfcoat.2014.08.072

Bernardes, L. J. L. (2006). Granulação de Materiais. *Cerâmica Ind.* 3-11, 17

Bhadeshia, H. K. D. H. (2001). *Bainite in Steels: Transformations, Microstructure and Properties.* 2ed. Londres: IOM Communications.

Binder, C., Bindo, T., Pereira, R. V., Hammes, G., de Mello, J. D. B., and Klein, A. N. (2016). Influence of the SiC Content and Sintering Temperature on the Microstructure, Mechanical Properties and Friction Behaviour of Sintered Self-Lubricating Composites. *Powder Metall.* 59-5, 384–393. doi:10.1080/00325899.2016.1250036

Binder, R. (2008). *Composition of Particulate Materials for Forming Self-Lubricating Products in Sintered Steels, Product in Self- Lubricating Sintered Steel and Process for Obtaining Self-Lubricating Products in Sintered Steel.* US 20110286873A1-USA. Alexandria, Virginia: The United States Patent and Trademark Office (USPTO).

Bralla, J. G. (1996). *Design for Excellence*. New York City: McGraw-Hill.

Campos, K. R., Kapsa, P., Binder, C., Klein, A. N., and de Mello, J. D. B. (2015). Tribological Evaluation of Self-Lubricating Sintered Steels. *Wear* 332, 932–940. doi:10.1016/j.wear.2015.01.056

Clayton, P., Sawley, K. J., Bolton, P. J., and Pell, G. M. (1987). Wear Behavior of Bainitic Steels. *Wear* 120, 199–220. doi:10.1016/0043-1648(87)90067-6

Damin, K. V. S., da RosaTasior, G., Lucena, A. C., Bendo, T., Hammes, G., Klein, A. N., et al. (2020). Improvement of Tribological Properties of Sintered Self-Lubricating Composites Produced by Surface Mo-Enrichment. *Wear* 442-443, 203123. doi:10.1016/j.wear.2019.203123

Damin, K. V. S. (2019). *Enriquecimento de compósitos autolubrificantes utilizando plasma DC*. Florianópolis SC: Universidade Federal de Santa

Catarina, In Portuguese. PhD Thesis https://repositorio.ufsc.br/handle/123456789/206473.

Damin, K. V. S., Lucena, A. C., Bendo, T., Klein, A. S., and Binder, C. (2019). Self-lubricating Composites Enriched in the Surface with Molybdenum and Nickel. *Mat. Res.* 22, 20180803, doi:10.1590/1980-5373-mr-2018-0803

De Mello, J. D. B., Binder, C., Hammes, G., Binder, R., and Klein, A. N. (2017). Tribological Behaviour of Sintered Iron Based Self Lubricating Composites. *Friction* 5-3, 285–307. doi:10.1007/s40544-017-0186-2

De Mello, J. D. B., Binder, C., Hammes, G., and Klein, A. N. (2013). Effect of the Metallic Matrix on the Sliding Wear of Plasma Assisted Debinded and Sintered MIM Self-Lubricating Steel. *Wear* 301, 648–655. doi:10.1016/j.wear.2013.01.011

De Mello, J. D. B., Binder, C., Klein, A. N., and Binder, R. (2010). Effect of Sintering Temperature on the Tribological Behavior of Plasma Assisted Debinded and Sintered MIM Self Lubricating Steels. *Asme 2010 10th Bienn. Conf. Eng. Syst. Des. Analysis* 1, 373–380. doi:10.1115/esda2010-24245

De Mello, J. D. B., and Binder, R. (2006). A Methodology to Determine Surface Durability in Multifunctional Coatings Applied to Soft Substrates. *Tribol. Int.* 39-8, 769–773. doi:10.1016/j.triboint.2005.07.015

Demetrio, V. B., et al. (2017). Development of the Self-Lubricating Steels by Compression of Granulated Powders. *Mater. Sci. Forum* 899, 299–304. doi:10.4028/www.scientific.net/msf.899.299

Dhanasekaran, S., and Gnanamoorthy, R. (2007). Microstructure Strength and Tribological Behavior of Fe–C–Cu–Ni Sintered Steels Prepared with MoS2 Addition. *J. Mat. Sci.* 42-12, 4659–4666. doi:10.1007/s10853-006-0385-0

Donnet, C., and Erdemir, A. (2008). *Tribology of Diamond-Like Carbon Films: Fundamentals and Applications*. New York: Springer.

Erdemir, A., and Donnet, C. (2006). Tribology of Diamond-like Carbon Films: Recent Progress and Future Prospects. *J. Phys. D Appl. Phys.* 39-18, 311–327. doi:10.1088/0022-3727/39/18/r01

Erdemir, A. (2015). Review of Engineered Tribological Interfaces for Improved Boundary Lubrication. *Tribol. Int.* 38-3, 249–256. doi:10.1016/j.triboint.2004.08.008

Erdemir, A. (2001). "Solid Lubricants and Self-Lubricating Films," in *BHUSHAN, B. Modern Tribology Handbook* (CRC Press, v. II), 787

Furlan, K. P., De mello, J. D., and Klien, A. L. (2018). Self-lubricating Composites Containing MoS2: A Review. *Tribol. Int.* 120, 280–298. doi:10.1016/j.triboint.2017.12.033

German, R. M. (1996). *Sintering Theory and Practice*. New York: John Wiley & Sons.

Hammes, G. (2006). *Modificação da composição química da superfície de componentes metálicos via pulverização catódica em plasma: projeto de equipamento e desenvolvimento de processo*. Master dissertation. Florianopolis. Universidade Federal de Santa Catarina, In Portuguese. Available at: http://repositorio.ufsc.br/xmlui/handle/123456789/89137.

Hammes, G., Mucelin, K. J., Gonçalves, P. C., Binder, C., Binder, R., Janssen, R., et al. (2017). Effect of Hexagonal Boron Nitride and Graphite on Mechanical and Scuffing Resistance of Self Lubricating Iron Based Composite. *Wear* 376-377, 1084–1090. doi:10.1016/j.wear.2017.01.115

Holmberg, K., Andersson, P., Nylund, N. O., Makela, K., and Erdemir, A. (2014). Global Energy Consumption Due to Friction in Trucks and Buses. *Tribol. Int.* 78, 94–114. doi:10.1016/j.triboint.2014.05.004

Holmberg, K., and Erdemir, A. (2017). Influence of Tribology on Global Energy Consumption, Costs and Emissions. *Friction* 5, 263–284. doi:10.1007/s40544-017-0183-5

Huang, C., Du, L., and Zhang, W. (2009). Effects of Solid Lubricant Content on the Microstructure and Properties of NiCr/Cr_3C_2–BaF_2CaF_2 Composite Coatings. *J. Alloys Compd.* 479, 777–784. doi:10.1016/j.jallcom.2009.01.062

International Center for Diffraction Data,JCPDS., (2004). *PCPDFWIN*, Version PDF-2. Newtown Square, PA: International Center for Diffraction Data.

Kalpakjian, S. (2014). *Manufacturing Engineering and Technology*. Singapore: Pearson Education South Asia Pte Ltd.

Klein, A. N., Cardoso, R. P., Pavanati, H. C., Binder, C., Maliska, A. M., Hammes, G., et al. (2013). DC Plasma Technology Applied to Powder Metallurgy: an Overview. *Plasma Sci. Technol.* 15, 70–81. doi:10.1088/1009-0630/15/1/12

Ma, Y., Liu, Y., Menon, O., and Tong, J. (2015). Evaluation of Wear Resistance of Friction Materials Prepared by Granulation. *ACS Appl. Mat. Interfaces.* 7, 22814–22820. doi:10.1021/acsami.5b04654

Mahathanabodee, S., Palathai, T., Raadnui, S., Tongsric, R., and Sombatsompop, N. (2014). Dry Sliding Wear Behavior of SS316L Composites Containing H-BN and MoS2 Solid Lubricants. *Wear* 316, 37–48. doi:10.1016/j.wear.2014.04.015

Merie, V. V., Candea, V., and Popa, C. (2011). The Influence of Nickel Content on the Properties of Fe-Based Friction Composite Materials. *Metal. Int.* 16-4, 93

Metal Powder Industry Federation, MPIF (2010). *Standard 51: Determination of Microindentation Hardness of Power Metallurgy Materials*. Sweden: Metal Powder Industry Federation,

Metal Powder Industry Federation, MPIF (2005). *Standard 52: Determination of Effective Case Depth of Ferrous Powder Metallurgy Products*. Sweden,

Miyoshi, K. (2007). *Solid Lubricants and Coatings for Extreme Environments: State-Of-The-Art Survey*. Cleveland: Nasa.

Miyoshi, K. (2001). *Solid Lubrication Fundamentals and Applications*. Boca Raton: CRC Pres.

Mônego, G., Da Silva, G. B. D., Hammes, G., De.Mello, J. D. B., Binder, C., and Klein, A. N. (2018). Development of Dry Self-Lubricating Sintered Composites Containing hBN and Graphite Granulated with PVA." in *Euro PM2018 Congress Proceedings*. Bilbao: European Powder Metallurgy Association.

Omrani, E., Rohatgi, P. K., and Menezes, P. L. (2017). *Tribology and Applications of Self-Lubricating Materials*. Boca Raton:: CRC Press.

Pavanati, H. C., Lourenço, J. M., Maliska, A. M., Klein, A. N., and Muzart, J. L. R. (2007). Ferrite Stabilisation Induced by Molybdenum Enrichment in the Surface of Unalloyed Iron Sintered in an Abnormal Glow Discharge. *Appl. Surf. Sci.* 253-23, 9105–9111. doi:10.1016/j.apsusc.2007.05.036

Reed, J. S. (1998). *Principles of Ceramics Processing*. New York: John Wiley & Sons.

Reeves, C. J., Menezees, P. L., Lovel, M. R., and Jen, T. C. (2015). The Influence of Surface Roughness and Particulate Size on the Tribological Performance of Bio-Based Multi-Functional Hybrid Lubricants. *Tribol. Int.* 88, 40–55. doi:10.1016/j.triboint.2015.03.005

Scharf, T. W., and Prasad, S. V. (2013). Solid Lubricants: A Review. *J. Mater. Sci.* 48-2, 511–531. doi:10.1007/s10853-012-7038-2

Schroeder, et al. (2015). Internal Lubricant as an Alternative to Coating Steels. *Met. Powder Rep.* 65-7, 24

Sharma, S. M., and Anand, A. (2016). Solid Lubrication in Iron Based Materials - A Review. *Tribol. Industry* 38-3, 318

Stachowiak, K. G. W., and Batchelor, A. W. (2001). *Engineering Tribology*. Oxford: Elsevier.

Su, Y., Zhang, Y., Song, J., and Hu, L. (2017). Tribological Behavior and Lubrication Mechanism of Self-Lubricating Ceramic/metal Composites: The Effect of Matrix Type on the Friction and Wear Properties. *Wear* 372-373, 130–138. doi:10.1016/j.wear.2016.12.005

Tang, H., Coa, K., Wu, Q., Li, C., Yang, X., and Yan, X. (2011). Synthesis and Tribological Properties of Copper Matrix Solid Self-Lubricant Composites Reinforced with $NbSe_2$ Nanoparticles. *Cryst. Res. Technol.* 46-2, 195–200. doi:10.1002/crat.201000499

Taylor, J. R. (1996). *Introduction to Error Analysis: The Study of Uncertainties in Physical Measurements*. California:: University of Science Book, 488.

Teisanu, C., and Gheorghe, S. (2011). Development of New PM Iron-Based Materials for Self-Lubricating Bearings. *Adv. Tribol.* 11, 248037. doi:10.1155/2011/248037

Thummler, F., and Oberacker, R. (1993). *An Introduction to Powder Metallurgy*. Londres: The Institute Of Materials.

Ünlü, B. S. (2011). Tribological and Mechanical Properties of PM Journal Bearings. *Powder Metal.* 54-3, 338–342. doi:10.1179/003258909X12553422176880

Velkavrh, I., Kalin, M., and Vizintin, J. (2008). The Performance and Mechanisms of DLC-Coated Surfaces in Contact with Steel in Boundary-Lubrication Conditions - A Review. *J. Mech. Eng. Strojniski Vestn.* 54, 189-206.

Wu, Y. X., Wanf, F., Cheng, Y., and Chen, N. (1997). A Study of the Optimisation Mechanism of Solid Lubricant Concentration in Ni/MoS2 Self-Lubricating Composite. *Wear* 205, 64–70. doi:10.1016/s0043-1648(96)07299-7

Xie, X., and Chen, M. (2015). *Suizhou Meteorite: Mineralogy and Shock Metamorphism*. Berlin: Springer-Verlag,

Yas', D. S., Pavlenko, V. I., and Podmokov, V. B. (1976). Metal-graphite Materials of High Graphite Content and Some Methods of Their Preparation. *Poroshkovaya Metall.* 1-157, 31–34. doi:10.1007/bf00792403

Yilmaz, S. S., Unulu, B. S., and Varol, R. (2010). Effect of Boronizing and Shot Peening in Ferrous Based FeCu–Graphite Powder Metallurgy Material on Wear Microstructure and Mechanical Properties. *Mater Des.* 31-9, 4496–4501. doi:10.1016/j.matdes.2010.04.028

Zhu, J., Ma, L., and Dwyer-Joyce, R. (2020). Friction and Wear Behaviours of Self-Lubricating Peek Composites for Articulating Pin Joints. *Tribol. Int.* 149, 105741. doi:10.1016/j.triboint.2019.04.025

Zhu, S., Bi, Q., Yang, J., Liu, W., and Xue, Q. (2011). Effect of Particle Size on Tribological Behaviour of Ni_3Al Matrix High Temperature Self-Lubricating Composites. *Tribol. Int.* 44, 1800–1809. doi:10.1016/j.triboint.2011.07.002

Conflict of Interest: The authors declare that the research was conducted in the absence of any commercial or financial relationships that could be construed as a potential conflict of interest.

Publisher's Note: All claims expressed in this article are solely those of the authors and do not necessarily represent those of their affiliated organizations, or those of the publisher, the editors, and the reviewers. Any product that may be evaluated in this article, or claim that may be made by its manufacturer, is not guaranteed or endorsed by the publisher.